crystals

MDPI

Article

Electrowetting and Surface Tension of Chromonic Liquid Crystals

Filippo Marinello [1], Davide Ferraro [1], Alessio Meggiolaro [1], Sebastian Cremaschini [1], Annamaria Zaltron [1], Matteo Pierno [1], Giampaolo Mistura [1,*], Giuliano Zanchetta [2] and Liana Lucchetti [3,*]

[1] Dipartimento di Fisica e Astronomia G. Galilei, Università di Padova, Via Marzolo 8, 35131 Padova, Italy; filippo.marinello@phd.unipd.it (F.M.); davide.ferraro@unipd.it (D.F.); alessio.meggiolaro@studenti.unipd.it (A.M.); sebastian.cremaschini@phd.unipd.it (S.C.); annamaria.zaltron@unipd.it (A.Z.); matteo.pierno@unipd.it (M.P.)
[2] Dipartimento di Biotecnologie Mediche e Medicina Traslazionale, Università di Milano, Via F.lli Cervi 93, 20054 Segrate, Italy; giuliano.zanchetta@unimi.it
[3] Dipartimento SIMAU, Universita' Politecnica delle Marche, Via Brecce Bianche, 60131 Ancona, Italy
* Correspondence: giampaolo.mistura@unipd.it (G.M.); l.lucchetti@univpm.it (L.L.)

Abstract: In this work, we report on measurements of the contact angle of sessile droplets of aqueous solutions of a chromonic liquid crystal at different temperatures and concentrations and on different hydrophobic surfaces, and we show that the wettability of this complex fluid can be easily controlled by an external electric field. Specifically, electrically induced variations of the contact angle up to 70° were obtained using external DC voltages. Complementary tensiometric measurements of the aqueous solutions confirmed that the observed variations in the contact angle were mainly related to variations in the surface tension, while they did not show an evident connection with the internal molecular order of the liquid crystal droplets. Our study is relevant in view of the use of chromonic liquid crystals in microfluidic devices, where the control of wettability is an important tool for handling fluid flow.

Keywords: chromonic liquid crystals; wetting; electrowetting

Citation: Marinello, F.; Ferraro, D.; Meggiolaro, A.; Cremaschini, S.; Zaltron, A.; Pierno, M.; Mistura, G.; Zanchetta, G.; Lucchetti, L. Electrowetting and Surface Tension of Chromonic Liquid Crystals. *Crystals* **2024**, *14*, 1. https://doi.org/10.3390/cryst14010001

Academic Editors: Shuxin Liu, Quanming Chen, Changli Sun and Kun Yin

Received: 30 November 2023
Revised: 15 December 2023
Accepted: 17 December 2023
Published: 19 December 2023

1. Introduction

Wetting is one of the fundamental phenomena in physical chemistry [1], affecting the shape and motion of liquid droplets on solid surfaces, fluid flows in confined geometries and the behavior of solid inclusions in liquids [2–4]. It is relevant in a wide range of applications in the biomedical, environmental and energy sectors. Controlling wettability, together with the possibility of obtaining superhydrophobic surfaces, has been extensively investigated for isotropic liquids, with particular emphasis on the influence of the chemical composition and roughness of the substrate [5,6], but much less is known for more complex fluids and surfaces.

The possibility of controlling the wettability by external electric fields, known as electrowetting, has also been extensively studied, and electrowetting is currently one of the most widely used tools for manipulating water droplets on surfaces [7,8]. Surprisingly, although complex fluids are known to be very sensitive to external stimuli, only a few studies on electrowetting of non-isotropic fluids are available [9,10].

Wetting is also particularly important for liquid crystals (LCs) and their applications [11–15], and its theory has been investigated over the years by many authors [16–21]. Despite this, very few systematic studies of the contact angle of LC sessile droplets are available [21–24] and little is known about their dynamic wetting. In recent years, there has been renewed interest in these phenomena [24–28], due to the discovery of new liquid-crystal phases [29] and to an increasing interest in the use of LCs as platforms for chemical and biological sensing [30,31].

In this work, we report on electrowetting experiments on sessile droplets of a lyotropic chromonic LC deposited on different passive surfaces and show that the droplet contact

angle can be efficiently controlled by an external DC electric field over a wide range of values.

Chromonics are a class of lyotropic LCs made of rigid, plank- or blade-shaped aromatic systems that are functionalised in the periphery with ionic or hydrophilic groups for solubility in aqueous media [32,33]. Such molecules, which also include short DNA duplexes and single nucleotides [34], form reversible aggregates, which, at sufficiently high concentrations, spontaneously align in the nematic (N) and columnar LC phases. The aggregates are bound by weak hydrophobic and π–π interactions, so their length varies strongly with concentration, temperature and ionic content, which is reflected in their phase diagram. Chromonics have been proposed as biosensors [35–38], as biomimetic vehicles for the delivery of soluble drugs or medical contrast agents [39] and for the rapid detection of pathogens [40]. Achieving good control of the contact angle of water-based chromonic liquid crystal droplets on different substrates is, thus, desirable in view of the variety of possible bioinspired applications, such as microfluidic biosensors or microtools for drug delivery.

2. Materials and Methods

As a chromonic LC, we used disodium cromoglycate (DSCG) dissolved in water at different weight concentrations (c) ranging from 4% to 13% (*wt*/*wt*). DSCG, also known as cromolyn, is an organic acid based on water. It is optically transparent and can be used as an antiasthmatic drug [41]. Its chemical formula is shown in Figure 1a. DSCG molecules in water assemble reversibly, forming elongated polydisperse aggregates. In the absence of condensing agents, the length of the aggregates is influenced by the temperature and volume fraction. For example, a pure DSCG solution with a weight concentration of 10% is isotropic (I) at temperatures $T > 33$ °C, as the aggregates are too short to form an orientationally ordered phase. In the range of 21 °C $< T <$ 33 °C, the solution exhibits a biphasic isotropic/nematic (I–N) region and is a homogeneous nematic (N) at $T <$ 21 °C [41]. DSCG was purchased as a powder from Sigma-Aldrich (C0399). For electrical control of the contact angle of sessile DSCG droplets, we used two different conducting substrates: a stainless-steel plate coated with a lubricant-infused surface (LIS) and a copper plate coated with microscopic layers of polydimethylsiloxane (PDMS). Lubricant-infused surfaces are made by textured materials imbibed with suitable oils [3,42,43]. Because lubricant surfaces are intrinsically smooth and free from the typical chemical and morphological defects of solid surfaces, they exhibit very low contact-line pinning and water droplets can easily move on them. This slippery character is exploited in various applications [3,44], including the study of droplets of highly viscous complex fluids, which barely move on solid surfaces [45,46]. The lubricant-infused surfaces used in the present work consisted of porous polytetrafluoroethylene (PTFE) membrane filters with high porosity (solid fraction $\phi_s \sim 0.16$, nominal size of the pores 0.2 μm, Sterlitech Corporation, Auburn, WA, USA), which were placed on the upper surface of a steel plate slide and wetted with ethanol to make them adhere smoothly by capillarity, see Figure 1b. Once the ethanol was evaporated, the membrane was impregnated with fluorinated oil (Fomblin PFPE (perfluoropolyether) Y LVAC (lubricant in vacuum) 06/6) with viscosity 120 mPa s and surface tension $\gamma = 21$ mN/m at $T = 20$ °C using a dip coater (Kibron Inc., Helsinki, Finland, LayerX 274). The withdrawal velocity during dip-coating was set at 0.12 mm/min to ensure a controlled thickness of the liquid layer above the membrane of ~0.5 μm (see ref. [47] for further details). The resulting LIS coatings had thicknesses of ~9 μm and ~25 μm. The PDMS was spin-coated on the copper plate at a speed of 3000 rpm. Before PDMS deposition, the copper electrode was carefully lapped until it reached surface roughness with rms value of about 10 nm, producing a PDMS coating with uniform thickness $d \sim 10$ μm, see Figure 1b.

Sessile droplets of DSCG of volume $\Omega = 5$ μL were deposited on the surfaces with a micropipette. A DC voltage was applied between the conducting plate (lower electrode) and a counter electrode made of a thin tungsten wire (diameter ~0.25 mm) slightly inserted into the droplet, as in Figure 1c,d. The contact angle of the droplet was measured by

analyzing backlight images of the contour of the droplet acquired by a CCD camera, as shown in Figure 1e,f, using a custom setup [48]. The temperature was controlled by means of a Peltier cell thermally coupled to the plates and measured with a thermocouple in contact with the conducting plate. The optical setup was also used for the measurement of the surface tension at different concentrations of aqueous DSCG solution and different temperatures with the pendant-drop method.

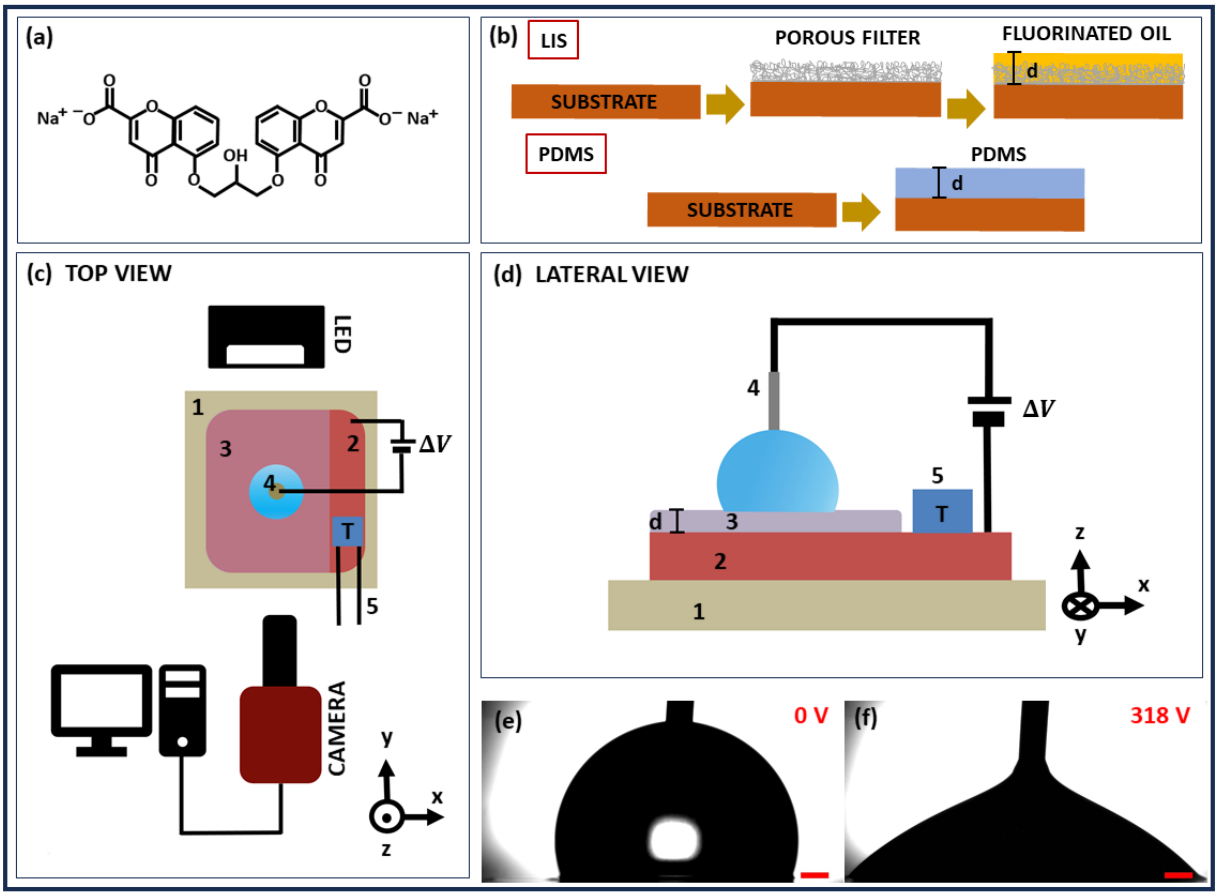

Figure 1. (**a**) Chemical formula of chromolin (DSCG). (**b**) Sketches of the conducting substrates coated with a lubricant-infused surface and with PDMS. (**c**) Top and (**d**) lateral views of the experimental setup: (1) Peltier cell, (2) lower electrode, (3) coating, (4) counter electrode and (5) thermocouple. Side view of a DSCG droplet at V = 0 V (**e**) and V = 318 V (**f**) on stainless steel coated with a LIS. The red lines correspond to 0.25 mm.

3. Results and Discussion

Electrowetting experiments on the LIS were performed on DSCG droplets with a fixed weight concentration c = 10%. Measurements were carried out at three different temperatures, T = 14, 22 and 35 °C, which corresponded to the nematic phase (N), the biphasic region (N + I) and the isotropic phase (I), respectively [32]. The measured contact angle θ of the sessile DSCG droplets is shown in Figure 2a as a function of the voltage ΔV applied between the electrodes. Each experimental point is the average of at least three measurements and the error bars correspond to one standard deviation.

Figure 2 shows a pronounced monotonic decrease in contact angle with applied voltage, indicating that the wettability of the DSCG droplets can be efficiently tuned by ΔV. In fact, at the maximum voltage ΔV = 350 V, the contact angle decreased by 70°. Interestingly, the three curves exhibit essentially the same shape and are just slightly vertically shifted with respect to one another. Specifically, no major variations related to the different degrees of molecular order in the DSCG could be detected and the origin of the vertical shift can

possibly be ascribed to the decrease of the surface tension with temperature. The small fluctuations for the high voltage values at T = 35 °C were probably caused by the shorter experimental runs required by the faster evaporation of the droplets at this temperature.

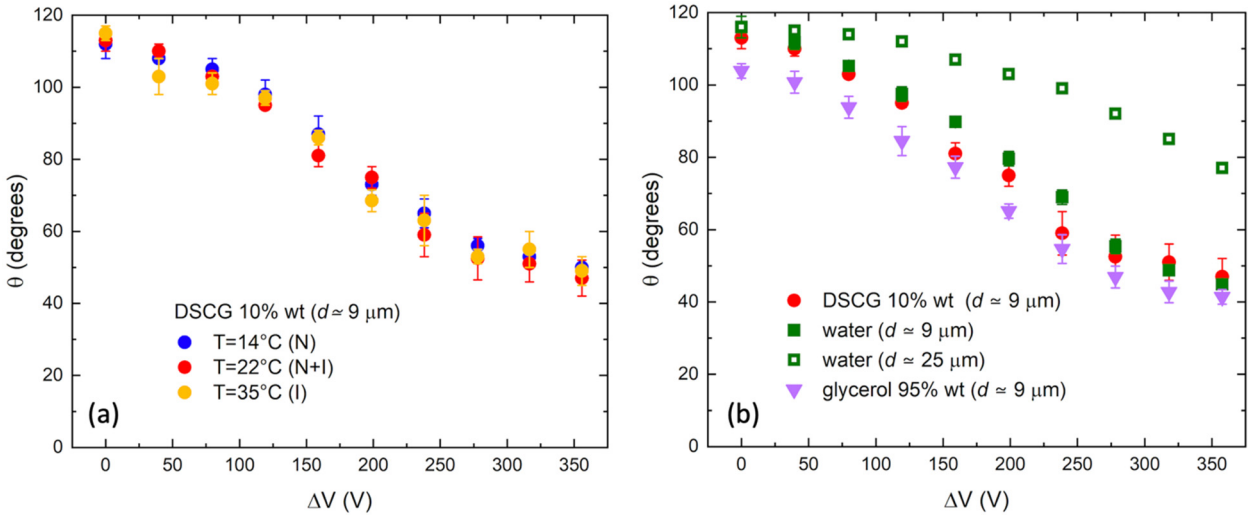

Figure 2. (**a**) Contact angle θ of DSCG sessile droplets with concentration c = 10% as a function of the voltage ΔV applied between the electrodes. Data refer to three different temperatures, which correspond to the nematic (N), mixed nematic–isotropic (N + I) and isotropic (I) phases. (**b**) Voltage dependence of the contact angle of the sessile DSCG droplets at c = 10%, compared with pure water and glycerol–water solution with c = 95%, measured at T = 22 °C. All data in Figure 2 refer to the same droplet volume Ω = 5 μm. The values of d in parentheses indicate the thickness of the LIS (see main text).

The wettability response of the DSCG droplets to an applied voltage was compared to that of the sessile droplets of simple liquids such as pure water, and an aqueous solution of glycerol at c = 95% weight, deposited on the same lubricant-infused surface at T = 22 °C. Data are shown in Figure 2b. The shape of the three curves is very similar, suggesting that the liquid crystalline nature of the DSCG droplets did not play a major role at the relevant length scales in our experimental conditions. Specifically, the curves related to the aqueous solution of DSCG and pure water are almost superimposed, while the one describing the behaviour of glycerol exhibits systematically lower values of θ, suggesting a lower value of the liquid/vapour surface tension γ. In general, the contact angle of sessile droplets deposited on the same substrate is directly related to γ [1,7]. The values of γ for the three systems, measured with the pendant-drop method [49] are reported in Table 1 (third column). At T = 22 °C, the values obtained are γ (water) = 72.7 ± 0.3 mN/m, γ (glycerol–water) = 60 ± 1 mN/m and γ (DSCG) = 71.0 ± 0.5 mN/m. These values are fully consistent with the curves in Figure 2b: the lower contact angles of the glycerol droplets reflect the lower surface tension of this solution.

The liquid/vapour surface tension can be independently evaluated by using the Lippmann equation, which describes the dependence of the contact angle on the applied voltage [7]:

$$\cos\theta = \cos\theta_0 + \frac{\epsilon_0 \epsilon_r}{2d\gamma}\Delta V^2 \quad (1)$$

In Equation (1), θ_0 is the contact angle in the absence of the external voltage, ϵ_0 and ϵ_r are the dielectric constants of the vacuum and of the dielectric layer on which the droplet is placed, respectively, d is the thickness of the dielectric layer and ΔV the applied voltage. The role played by d is clear in Figure 2b, where two θ vs. ΔV curves for sessile water droplets measured on two different LISs having different thicknesses, are shown (full squares and open squares). As expected, the electrically induced decrease in the contact angle is much lower in the case of a thicker dielectric coating.

According to the Lippmann formula, a linear fit of the curve $cos\ \theta$ vs. ΔV^2 allows γ to be extracted from the resulting slope $\frac{\epsilon_0 \epsilon_r}{2d\gamma}$. Figure 3 shows the cos θ vs. ΔV^2 curve for DSCG droplets at the three temperatures used in Figure 2a. As an example, the straight line represents the least-squares linear fit of the curve corresponding to T = 14 °C, determined by discarding the last points at high voltages, where the contact angle is close to saturation [7]. Under our experimental conditions, the LIS acts as a dielectric layer with an effective ϵ_r, which can be estimated as a weighted average between the dielectric permittivity of the membrane and that of the lubricant: $\epsilon_r \sim \phi_s \epsilon_{PTFE} + (1 - \phi_s)\epsilon_{oil}$. Assuming the following values for the PTFE membrane and oil, $\epsilon_{PTFE} \sim 2.1$, $\epsilon_{oil} \sim 2.2$ and $\phi_s \sim 0.16$, one obtains $\epsilon_r \sim 2.2$. The values of γ estimated in this way are listed in the last column of Table 1.

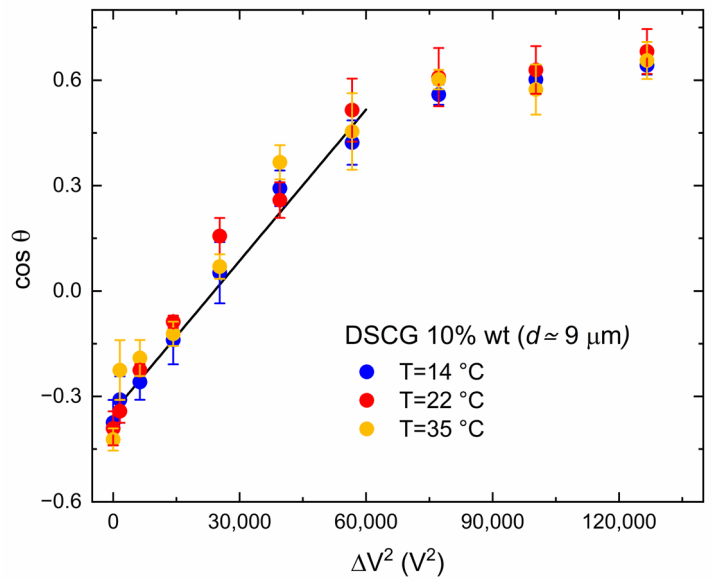

Figure 3. Cosine of the contact angle as a function of the square of the voltage applied between the electrodes. Data refer to an aqueous solution of DSCG with $c = 10\%$, on the LIS. The black line is the best fit of the curve corresponding to T = 14 °C.

The large experimental errors are a consequence of both those affecting the parameters used to calculate the liquid/vapour surface tension (see Equation (1)) and of the intrinsic difficulty in defining a uniform thickness d for the LIS. Nevertheless, the data are fully consistent, within the experimental uncertainties, with the corresponding values measured directly with the pendant-drop method.

Table 1. Surface tensions of the liquids used in this study directly measured at different temperatures with the pendant-drop method or estimated by the Lippman equation.

Solution	T (°C)	γ (mN/m) Pendant Drop	Surface	γ (mN/m) Linear Fit
Water	22	72.7 ± 0.3	LIS	71 ± 6
Glycerol–water 95%	22	60 ± 1	LIS	67 ± 7
DSCG–water 10%	14	75 ± 1	LIS	68 ± 7
DSCG–water 10%	22	71.0 ± 0.5	LIS	64 ± 6
DSCG–water 10%	35	69 ± 1	LIS	68 ± 6
Water	22	72.7 ± 0.3	PDMS	74 ± 5
DSCG–water 4%	22	72.6 ± 0.7	PDMS	72 ± 4
DSCG–water 6%	22	72.0 ± 0.7	PDMS	68 ± 6
DSCG–water 8%	22	71.7 ± 0.3	PDMS	75 ± 6
DSCG–water 10%	22	71.0 ± 0.5	PDMS	71 ± 5
DSCG–water 13%	22	68.5 ± 0.8	PDMS	64 ± 4

Similar measurements were repeated on the PDMS-coated copper plate. PDMS is widely used for the fabrication and prototyping of microfluidic chips, which makes the possibility of controlling the contact angle of DSCG sessile droplets on this substrate particularly interesting. In this case, the contact angle was measured for different DSCG concentrations c, with the temperature fixed at T = 22 °C (Figure 4a). Under these experimental conditions, DSCG was in the biphasic region (N + I) for all values of c. The maximum applied voltage in these measurements was limited to 200 V to avoid electrolysis of the DSCG droplets. It should be noted that the contact angle of pure water droplets in the absence of applied voltage was slightly lower than that measured on the LIS, 108° ± 2° vs. 116° ± 3°, reflecting the different hydrophobic nature of the two surfaces.

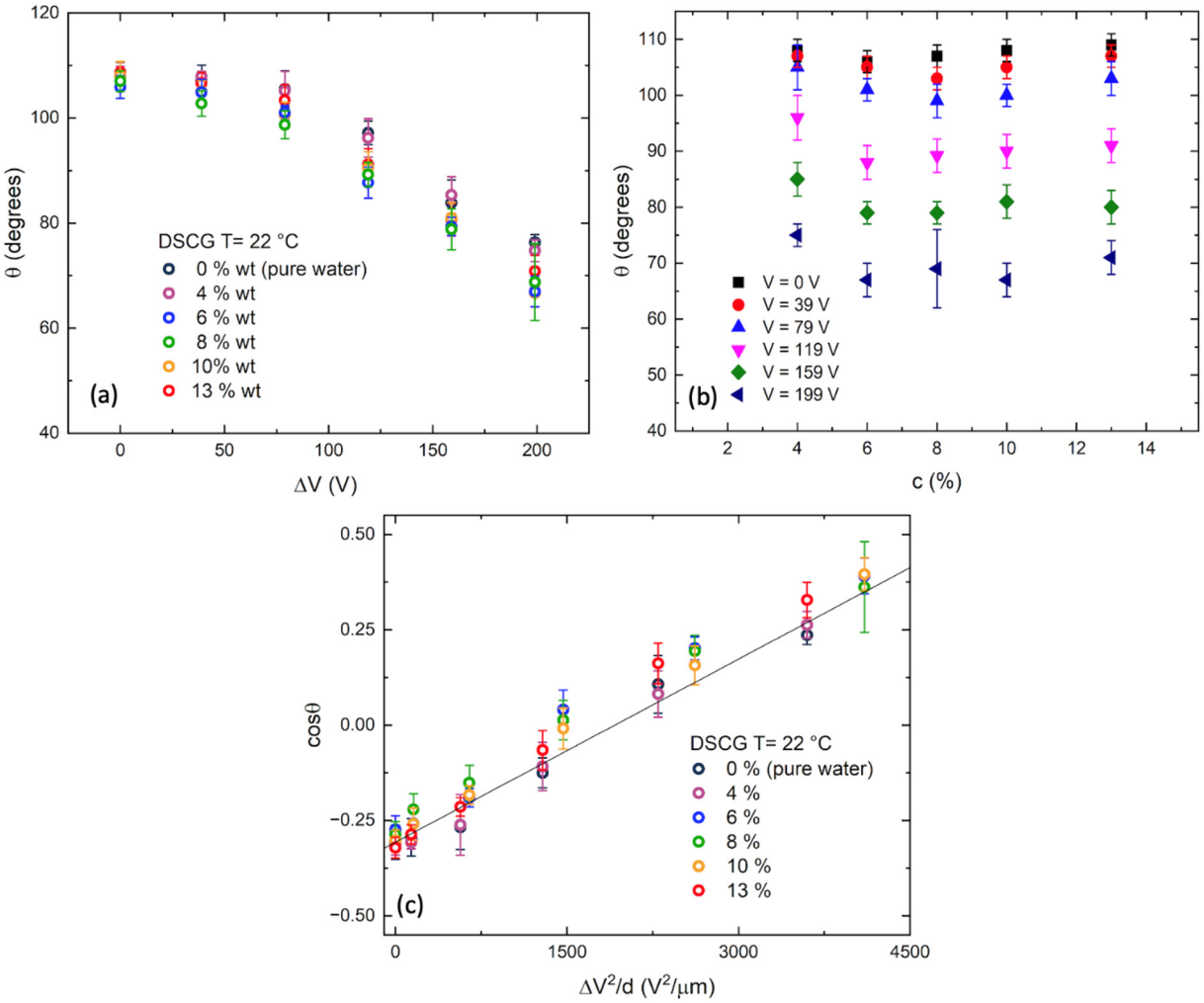

Figure 4. (**a**) Contact angle θ of sessile DSCG droplets on PDMS as a function of the voltage ΔV, for different values of the concentration. (**b**) Contact angle θ as a function of the DSCG weight concentration c, for different values of the applied voltage ΔV. (**c**) Cosine of the contact angle θ of the sessile DSCG droplets at different weight concentrations as a function of the applied squared voltage ΔV^2 normalised by the thicknesses d of the PDMS coatings. The black line represents the behaviour of pure water droplets determined using the Lippman equation.

Experimental data clearly show that θ could also be efficiently electrically tuned on PDMS for each of the DSCG concentrations considered. Figure 4a does not reveal a strong effect of concentration. To further analyse this point, θ, as a function of c, was extracted from the experimental data and is reported in Figure 4b, for different values of the applied voltage. Apart from the decrease in θ upon increasing ΔV, no specific dependence of the contact angle on c was observed, which seems to indicate an unexpected very weak

dependence of the DSCG surface tension on the concentration. It is noteworthy that a very weak surface activity of DSCG had already been reported in [50] where this chromonic LC was investigated as a cell membrane stabiliser and did not cause any measurable decrease in surface tension when added to the monolayer and bilayers of phospholipids at different concentrations. On the contrary, a slight increase in surface tension with concentration has been reported for the different chromonic molecule sunset yellow [51].

The surface tension of the DSCG droplets, as a function of c, was measured directly with the pendant-drop method [48] and the values obtained are reported in Table 1. Data show only a weak decrease in γ on increasing c. For completeness and in analogy to the LIS, we also determined the surface tension through the linear fit of the cosθ vs. ΔV^2 curves, see Figure 4c. In this case, to facilitate comparison among data taken on different PDMS coatings, the voltage was normalised to the thickness d of the corresponding PDMS film, measured with a profilometer. The straight line in the figure is not the best fit, but rather the prediction of the Lippmann equation for pure water droplets. The graph clearly shows that the wettability data of the DSCG droplets essentially follow this linear trend, which is an additional indication that the presence of DSCG does not dramatically affect the contact angle behaviour. The values of γ estimated by fitting the curves in Figure 4b, assuming a PDMS dielectric constant $\epsilon_r \sim 2.7$, are also reported in Table 1 (last column). As expected, the data did not show any clear dependence on c. Indeed, the weak decrease in the surface tension with concentration, observed with the direct measurement of γ, did not reflect in the behaviour of the contact angle observed in Figure 4a, which was instead substantially independent of c.

We point out that the measured DSCG surface tension, close to that of pure water, is higher than that of typical thermotropic nematic LCs, such as, for example, 5CB and other cyanobiphenyls or cyanophenylbenzoates, whose surface tension is known to be around 20–30 mN/m [52,53]. Nonetheless, the formation of nematic tactoids in DSCG, when a proper concentration of PEG is added to the water solution, has been reported [54]. The slender shape of these inclusions has been attributed to a relatively small interfacial tension compared with thermotropic liquid crystals, which usually form spherical inclusions in isotropic fluids [54]. The apparent disagreement between our findings and ref. [54] suggests that DSCG surface tension is very sensitive to the presence of dopants in the water solution, which offers an additional degree of freedom for the control of wettability of this liquid crystalline system.

4. Conclusions

We reported on the possibility of tuning the contact angle of DSCG sessile droplets by an external voltage in an electrowetting configuration. The control of wettability achieved in electrowetting experiments was quite efficient both on the LIS and on PDMS, leading to a variation of the contact angle $\Delta\theta$ as high as 70° for applied voltages of 350 V.

Electrowetting experiments at different concentrations highlighted that the contact angle of sessile DSCG droplets did not show any pronounced dependence on this parameter, at least in our experimental conditions. Direct measurements of the liquid/vapour surface tension revealed only a very weak decrease with increasing concentration, a dependence that, however, does not reflect in the behaviour of the contact angle, probably masked by the errors associated to the determination of θ.

Our results allow us to extend the use of a robust technique of wetting control, such as electrowetting, to this intriguing class of liquid crystalline systems. Chromonics are indeed stable and soluble in aqueous media and, thus, suitable for biological applications. Therefore, the ability to control their wettability is desirable for a variety of possible uses, from biosensors to biomimetic vehicles for drug delivery. For instance, liquid crystal droplets with a properly functionalised surface have recently been proposed as optical biosensors, since biomolecules adsorbed on the droplet surface can trigger liquid crystal reorientation [55]. Sessile droplets of DSCG with electrically controlled wettability might,

thus, be used as optical biosensors moving along specific paths on a microfluidic platform with patterned electrodes.

A possible further development of the reported study may foresee the use of photoactive lithium niobate crystals as droplet substrates for light control of DSCG wettability [24–26,47]. The use of lithium niobate platforms for droplet manipulation has indeed been recently demonstrated both for water [47] and for thermotropic liquid crystals [24–26].

Author Contributions: L.L. and G.M. designed the research; F.M., D.F., A.M., S.C., A.Z., M.P. and G.Z. performed the research; F.M., G.M. and L.L. analysed the data; G.M. and L.L. wrote the paper with input from all authors. All authors have read and agreed to the published version of the manuscript.

Funding: This research was partially funded by PRIN2017 UTFROM of the Italian Ministry of University and Research, by the BIRD Grant BIODIVSEQ and by the STARS Grant EXODROP of Padua University.

Data Availability Statement: Data are contained within the article.

Acknowledgments: The authors are particularly grateful to Giorgio Delfitto for his valuable technical assistance.

Conflicts of Interest: The authors declare no conflict of interest.

References

1. De Gennes, P.G.; Brochard-Wyart, F.; Quéré, D. *Capillarity and Wetting Phenomena: Drops, Bubbles, Pearls, Waves*; Springer: New York, NY, USA, 2004.
2. Bocquet, L.; Charlaix, E. Nanofluidics, from bulk to interfaces. *Chem. Soc. Rev.* **2010**, *39*, 1073–1095. [CrossRef] [PubMed]
3. Mistura, G.; Pierno, M. Drop mobility on chemically heterogeneous and lubricant-impregnated surfaces. *Adv. Phys.-X* **2017**, *2*, 591–607. [CrossRef]
4. Malinowski, R.; Parkin, I.P.; Volpe, G. Advances towards programmable droplet transport on solid surfaces and its applications. *Chem. Soc. Rev.* **2020**, *49*, 7879–7892. [CrossRef] [PubMed]
5. Roach, P.; Shirtcliffe, N.J.; Newton, M.I. Progess in superhydrophobic surface development. *Soft Matter* **2008**, *4*, 224–240. [CrossRef] [PubMed]
6. Nishimoto, S.; Bhushan, B. Bioinspired self-cleaning surfaces with superhydrophobicity, superoleophobicity, and superhydrophilicity. *RSC Adv.* **2013**, *3*, 671–690. [CrossRef]
7. Mugele, F.; Baret, J.C. Electrowetting: From basics to applications. *J. Phys. Condens. Matter* **2005**, *17*, R705–R774. [CrossRef]
8. Li, J.; Kim, C.J. Current commercialization status of electrowetting-on-dielectric (EWOD) digital microfluidics. *Lab Chip* **2020**, *20*, 1705–1712. [CrossRef]
9. Banpurkar, A.G.; Duits, M.H.G.; van den Ende, D.; Mugele, F. Electrowetting of Complex Fluids: Perspectives for Rheometry on Chip. *Langmuir* **2009**, *25*, 1245–1252. [CrossRef]
10. Mampallil, D.; Eral, H.B.; van den Ende, D.; Mugele, F. Control of evaporating complex fluids through electrowetting. *Soft Matter* **2012**, *8*, 10614–10617. [CrossRef]
11. Cheng, C.C.; Chang, C.A.; Yeh, J.A. Variable focus dielectric liquid droplet lens. *Opt. Express* **2006**, *14*, 4101–4106. [CrossRef]
12. Fan, S.K.; Chiu, C.P.; Lin, J.W. Electrowetting on polymer dispersed liquid crystal. *Appl. Phys. Lett.* **2009**, *94*, 164109. [CrossRef]
13. Wells, G.G.; Matranga, M.A.; Newton, C.J.P.; Taphouse, T.S.; Baig, S.A.; Kitson, S.C. Electrowetting pixels with improved transmittance using dye doped liquid crystals. *Appl. Phys. Lett.* **2013**, *103*, 031107. [CrossRef]
14. Fukuto, M.; Gang, O.; Alvine, K.J.; Ocko, B.M.; Pershan, P.S. Wetting of liquid-crystal surfaces and induced smectic layering at a nematic-liquid interface: An x-ray reflectivity study. *Phys. Rev. E* **2008**, *77*, 031607. [CrossRef] [PubMed]
15. Liu, I.B.; Gharbi, M.A.; Ngo, V.L.; Kamien, R.D.; Yang, S.; Stebe, K.J. Elastocapillary interactions on nematic films. *Proc. Natl. Acad. Sci. USA* **2015**, *112*, 6336–6340. [CrossRef]
16. Teixeira, P.I.C.; Sluckin, T.J.; Sullivan, D.E. Landau-De Gennes theory of anchoring transitions at a nematic liquid-crystal substrate interface. *Liq. Cryst.* **1993**, *14*, 1243–1253. [CrossRef]
17. Delrio, E.M.; Dagama, M.M.T.; Demiguel, E.; Rull, L.F. Surface-induced alignment at model nematic interfaces. *Phys. Rev. E* **1995**, *52*, 5028–5039. [CrossRef]
18. Osipov, M.A.; Sluckin, T.J.; Cox, S.J. Influence of permanent molecular dipoles on surface anchoring of nematic liquid crystals. *Phys. Rev. E* **1997**, *55*, 464–476. [CrossRef]
19. Rey, A.D.; Golmohammadi, M.; Valencia, E.E.H. A model for mesophase wetting thresholds of sheets, fibers and fiber bundles. *Soft Matter* **2011**, *7*, 5002–5009. [CrossRef]
20. Rey, A.D.; Herrera-Valencia, E.E. Dynamic wetting model for the isotropic-to-nematic transition over a flat substrate. *Soft Matter* **2014**, *10*, 1611–1620. [CrossRef]

21. Vanzo, D.; Ricci, M.; Berardi, R.; Zannoni, C. Wetting behaviour and contact angles anisotropy of nematic nanodroplets on flat surfaces. *Soft Matter* **2016**, *12*, 1610–1620. [CrossRef]
22. Hiltrop, K.; Stegemeyer, H. Contact angles and alignment of liquid crystals on lecithin monolayers. *Mol. Cryst. Liq. Cryst.* **1978**, *49*, 61–65. [CrossRef]
23. Gvozdovskyy, I.; Kurioz, Y.; Reznikov, Y. Exposure and temperature dependences of contact angle of liquid crystals on photoaligning surface. *Opto-Electron. Rev.* **2009**, *17*, 116–119. [CrossRef]
24. Barboza, R.; Marni, S.; Ciciulla, F.; Mir, F.A.; Nava, G.; Caimi, F.; Zaltron, A.; Clark, N.A.; Bellini, T.; Lucchetti, L. Explosive electrostatic instability of ferroelectric liquid droplets on ferroelectric solid surfaces. *Proc. Natl. Acad. Sci. USA* **2022**, *119*, e2207858119. [CrossRef] [PubMed]
25. Marni, S.; Barboza, R.; Zaltron, A.; Lucchetti, L. Optical control of mass ejection from ferroelectric liquid droplets: A possible tool for the actuation of complex fluids. *J. Mol. Liq.* **2023**, *384*, 122287. [CrossRef]
26. Marni, S.; Nava, G.; Barboza, R.; Bellini, T.G.; Lucchetti, L. Walking ferroelectric liquid droplets with light. *Adv. Mater.* **2023**, *35*, 2212067. [CrossRef] [PubMed]
27. Kolacz, J.; Wei, Q.H. Self-Localized Liquid Crystal Micro-Droplet Arrays on Chemically Patterned Surfaces. *Crystals* **2022**, *12*, 13. [CrossRef]
28. Ulaganathan, V.; Sengupta, A. Spatio-temporal programming of lyotropic phase transition in nanoporous microfluidic confinements. *J. Colloid Interface Sci.* **2023**, *649*, 302–312. [CrossRef]
29. Chen, X.; Korblova, E.; Dong, D.P.; Wei, X.Y.; Shao, R.F.; Radzihovsky, L.; Glaser, M.A.; Maclennan, J.E.; Bedrov, D.; Walba, D.M.; et al. First -principles experimental demonstration of ferroelectricity in a thermotropic nematic liquid crystal: Polar domains and striking electro-optics. *Proc. Natl. Acad. Sci. USA* **2020**, *117*, 14021–14031. [CrossRef]
30. Woltman, S.J.; Jay, G.D.; Crawford, G.P. Liquid-crystal materials find a new order in biomedical applications. *Nat. Mater.* **2007**, *6*, 929–938. [CrossRef]
31. Carlton, R.J.; Hunter, J.T.; Miller, D.S.; Abbasi, R.; Mushenheim, P.C.; Tan, L.N.; Abbott, N.L. Chemical and biological sensing using liquid crystals. *Liq. Cryst. Rev.* **2013**, *1*, 29–51. [CrossRef]
32. Lydon, J. Chromonic review. *J. Mater. Chem.* **2010**, *20*, 10071–10099. [CrossRef]
33. Tam-Chang, S.W.; Huang, L.M. Chromonic liquid crystals: Properties and applications as functional materials. *Chem. Commun.* **2008**, *17*, 1957–1967. [CrossRef]
34. Smith, G.P.; Fraccia, T.P.; Todisco, M.; Zanchetta, G.; Zhu, C.H.; Hayden, E.; Bellini, T.; Clark, N.A. Backbone-free duplex-stacked monomer nucleic acids exhibiting Watson-Crick selectivity. *Proc. Natl. Acad. Sci. USA* **2018**, *115*, E7658–E7664. [CrossRef]
35. Shiyanovskii, S.V.; Lavrentovich, O.D.; Schneider, T.; Ishikawa, T.; Smalyukh, I.I.; Woolverton, C.J.; Niehaus, G.D.; Doane, K.J. Lyotropic chromonic liquid crystals for biological sensing applications. *Mol. Cryst. Liq. Cryst.* **2005**, *434*, 259–587. [CrossRef]
36. Shiyanovskii, S.V.; Schneider, T.; Smalyukh, I.I.; Ishikawa, T.; Niehaus, G.D.; Doane, K.J.; Woolverton, C.J.; Lavrentovich, O.D. Real-time microbe detection based on director distortions around growing immune complexes in lyotropic chromonic liquid crystals. *Phys. Rev. E* **2005**, *71*, 020702. [CrossRef] [PubMed]
37. Woolverton, C.J.; Gustely, E.; Li, L.; Lavrentovich, O.D. Liquid crystal effects on bacterial viability. *Liq. Cryst.* **2005**, *32*, 417–423. [CrossRef]
38. Helfinstine, S.L.; Lavrentovich, O.D.; Woolverton, C.J. Lyotropic liquid crystal as a real-time detector of microbial immune complexes. *Lett. Appl. Microbiol.* **2006**, *43*, 27–32. [CrossRef] [PubMed]
39. de Souza, J.F.; Pontes, K.D.; Alves, T.F.R.; Amaral, V.A.; Rebelo, M.D.; Hausen, M.A.; Chaud, M.V. Spotlight on biomimetic systems based on lyotropic liquid crystal. *Molecules* **2017**, *22*, 419. [CrossRef] [PubMed]
40. Oton, E.; Oton, J.M.; Cano-Garcia, M.; Escolano, J.M.; Quintana, X.; Geday, M.A. Rapid detection of pathogens using lyotropic liquid crystals. *Opt. Express* **2019**, *27*, 10098–10107. [CrossRef] [PubMed]
41. Lee, H.; Labes, M.M. Phase diagram and thermodynamic properties of disodium cromoglycate-water lyomesophases. *Mol. Cryst. Liq. Cryst.* **1983**, *91*, 53–58. [CrossRef]
42. Lafuma, A.; Quere, D. Slippery pre-suffused surfaces. *Europhys. Lett.* **2011**, *96*, 56001. [CrossRef]
43. Wong, T.-S.; Kang, S.H.; Tang, S.K.Y.; Smythe, E.J.; Hatton, B.D.; Grinthal, A.; Aizenberg, J. Bioinspired self-repairing slippery surfaces with pressure-stable omniphobicity. *Nature* **2011**, *477*, 443–447. [CrossRef] [PubMed]
44. Li, J.S.; Ueda, E.; Paulssen, D.; Levkin, P.A. Slippery lubricant-infused surfaces: Properties and emerging applications. *Adv. Funct. Mater.* **2019**, *29*, 1802317. [CrossRef]
45. Sartori, P.; Ferraro, D.; Dassie, M.; Meggiolaro, A.; Filippi, D.; Zaltron, A.; Pierno, M.; Mistura, G. Oscillatory motion of viscoelastic drops on slippery lubricated surfaces. *Commun. Phys.* **2022**, *5*, 81. [CrossRef]
46. Carneri, M.; Ferraro, D.; Azarpour, A.; Meggiolaro, A.; Cremaschini, S.; Filippi, D.; Pierno, M.; Zanchetta, G.; Mistura, G. Sliding and rolling of yield stress fluid droplets on highly slippery lubricated surfaces. *J. Colloid Interface Sci.* **2023**, *644*, 487–495. [CrossRef]
47. Zaltron, A.; Ferraro, D.; Meggiolaro, A.; Cremaschini, S.; Carneri, M.; Chiarello, E.; Sartori, P.; Pierno, M.; Sada, C.; Mistura, G. Optofluidic platform for the manipulation of water droplets on engineered LiNbO3 surfaces. *Adv. Mater. Interfaces* **2022**, *9*, 2200345. [CrossRef]
48. Meggiolaro, A.; Cremaschini, S.; Ferraro, D.; Zaltron, A.; Carneri, M.; Pierno, M.; Sada, C.; Mistura, G. Determination of the dielectrophoretic force induced by the photovoltaic effect on lithium niobate. *Micromachines* **2022**, *13*, 316. [CrossRef]

49. Berry, J.D.; Neeson, M.J.; Dagastine, R.R.; Chan, D.Y.C.; Tabor, R.F. Measurement of surface and interfacial tension using pendant drop tensiometry. *J. Colloid Interface Sci.* **2015**, *454*, 226–237. [CrossRef]
50. Arakawa, K.; Tonooka, M.; Sakamoto, K. Membrane stabilizing action of NCO-650 and its congeners. *Jpn. J. Pharmacol.* **1984**, *36*, 311–318. [CrossRef]
51. Davidson, Z.S.; Huang, Y.; Gross, A.; Martinez, A.; Still, T.; Zhou, C.; Collings, P.J.; Kamien, R.D. Nat. *Commun.* **2017**, *8*, 15642.
52. Gannon, M.G.J.; Faber, T.E. The surface tension of nematic liquid crystals. *Philos. Mag. A* **1978**, *37*, 117–135. [CrossRef]
53. Korjenevsky, V.A.; Tomilin, M.G. Experimental investigation of the surface energy of a nematic liquid crystal. *Liq. Cryst.* **1993**, *385*, 643–649. [CrossRef]
54. Tortora, L.; Lavrentovich, O.D. Chiral symmetry breaking by spatial confinement in tactoidal droplets of lyotropic chromonic liquid crystals. *Proc. Natl. Acad. Sci. USA* **2011**, *108*, 5163–5168. [CrossRef] [PubMed]
55. Wang, Z.; Xu, T.; Noel, A.; Chen, Y.-C.; Liu, T. Applications of liquid crystals in biosensing. *Soft Matter* **2021**, *17*, 4675. [CrossRef]